HHS Public Access

Author manuscript

Nat Microbiol. Author manuscript; available in PMC 2020 December 08.

Published in final edited form as:

Nat Microbiol. 2020 September ; 5(9): 1134–1143. doi:10.1038/s41564-020-0737-6.

A Nutrient-limited Screen Unmasks Rifabutin Hyperactivity for XDR *Acinetobacter baumannii*

B. Luna[1,*], **V. Trebosc**[2], **B. Lee**[1], **M. Bakowski**[3], **A. Ulhaq**[1], **J. Yan**[1], **P. Lu**[1], **J. Cheng**[1], **T. Nielsen**[1], **J. Lim**[1], **W. Ketphan**[1], **H. Eoh**[1], **C. McNamara**[3], **N. Skandalis**[4], **R. She**[5], **C. Kemmer**[2], **S. Lociuro**[2], **G. E. Dale**[2], **B. Spellberg**[6,*]

[1]Department of Molecular Microbiology and Immunology, USC Keck School of Medicine, Los Angeles, CA 90033, USA. [2]BioVersys AG, Basel, Switzerland. [3]Calibr, a division of The Scripps Research Institute, La Jolla, CA 92037, USA. [4]Department of Medicine, USC Keck School of Medicine, Los Angeles, CA 90033, USA. [5]Department of Pathology, USC Keck School of Medicine, Los Angeles, CA 90033, USA. [6]Los Angeles County+University of Southern California Medical Center, Los Angeles, CA 90033, USA.

Abstract

Industry screens of large chemical libraries traditionally have relied on rich media to ensure rapid bacterial growth in high-throughput testing. We used eukaryotic, nutrient-limited growth media in a compound screen that unmasked a previously unknown hyper-activity of the old antibiotic, rifabutin (RBT), against highly resistant *Acinetobacter baumannii*. In nutrient-limited, but not rich media, RBT was 200-fold more potent than rifampin (RIF). RBT was also substantially more effective *in vivo*. The mechanism of enhanced efficacy was a Trojan horse-like import of RBT but not RIF through *FhuE*, only in nutrient-limited conditions. These results are of fundamental importance to efforts to discover antibacterial agents.

Discovery of new antibiotics has traditionally occurred via high throughput screening assays. These assays use rich media, such as Mueller-Hinton II (MHII) broth, to enable rapid microbial growth to facilitate the efficiency of the screens. Unfortunately, such methods rarely identify any new candidates.[1-5,7] However, we hypothesized that modifying the screening methodology by changing the media to be more reflective of the *in vivo* environment could uncover new activity of drugs with previously unknown efficacy. To test this hypothesis, we designed a nutrient-limited screen using media, more reflective of the *in vivo* environment. We sought to identify new antibiotics active against *Acinetobacter baumannii,* one of the most drug resistant bacterial pathogens, which is listed as the top

*Correspondence to: brian.luna@usc.edu and bradspellber@usc.edu.

Author contributions: BL, MB, VT, CM, and BS designed the experiments and wrote the manuscript. MB and CM helped design the HTS assay and performed the compound screening and analysis. BL, AU, JY, TN, PL, JL, JC, WK, HE, NS, RS, CK, SL, and GD participated in performing experiments, contributed intellectually, and interpreted results. BL, AU, PL, RS conducted the MIC testing. JL, WK, and HE conducted the LC-MS/MS experiments. JY, TBN, PL, and BL conducted the *in vivo* experiments.

Competing Interests: B.L., B.S. and T.N. own equity in ExBaq. The University of Southern California has a financial interest in ExBaq. G.E.D., V.T., C.K. and S.L. own equity in BioVersys.

priority of unmet need for new antibiotics by the World Health Organization.[6] Blood or lung infections caused by extreme drug resistant (XDR) *A. baumannii* cause >50% mortality,[8] and the antimicrobial pipeline for such infections is inadequate.[9-13]

The ReFRAME compound drug repurposing library[14] was screened against our well-characterized XDR, hyper-virulent clinical isolate of *A. baumannii* HUMC1.[15-19] As the growth media for our screen, we selected Roswell Park Memorial Institute medium (RPMI), a defined eukaryotic growth medium containing glucose (2 g/L) as the only carbon source, and mineral salts. We supplemented the RPMI with serum to better simulate the bloodstream environment.[20,21] Previous studies have identified the positive benefits of screening for antimicrobial compounds in culture conditions that are more reflective of conditions found *in vivo*[7,22,23].

In total we screened 11,862 small molecules at 20 μM (Supplementary Data File 1). The screen resulted in a hit rate of 0.52%; 62 putative hits were identified for follow-up confirmation in a serial dose response screen. About half of the compounds (32/62) were validated to inhibit 50% of bacterial growth (IC_{50}) at a concentration of less than 20 μM. These compounds were also assessed for half maximal mammalian cell cytotoxicity (CC_{50}), and 4 compounds had a favorable specific antibacterial activity (IC_{50} <20μM) and high selectivity (CC_{50}/IC_{50} > 10); of these rifabutin (RBT) was the most potent (i.e., had the lowest IC_{50}s, Fig. 1A).

We confirmed the superiority of RBT IC_{50} values in RPMI media, compared to a panel of 8 rifamycins, using a more sensitive, 11-point dose response curve (Fig. 1B). RBT was also confirmed to be the most potent and the least toxic rifamycin tested (Fig. 1C).

The minimum inhibitory concentration (MIC) of each drug was determined against *A. baumannii* HUMC1, a hyper-virulent, carbapenem-resistant, XDR strain. In nutrient-limited RPMI, the MIC of RBT (0.0156 μg/mL) was 200-fold lower as compared to RIF (3.125 μg/mL) (Fig. 1E). However, there was no difference in MIC when the bacteria were cultured in nutrient-rich MHII (MIC=3.125 μg/mL for both RBT and RIF) (Fig 1D). In contrast to *A. baumannii,* we did not find a universal improvement of RBT potency against other bacterial species tested (Fig. 1D, Extended Data Fig. 1).

We sought to understand the drivers responsible for the change in RBT potency in RPMI versus MHII media. Modulating the growth rate (temperature), carbon metabolism (glucose supplementation), or activity of cellular efflux pumps (efflux pump inhibitors) did not affect the MIC shift in nutrient-rich vs. -limited media. (Table 1). To distinguish if the discrepant RBT MICs in RPMI vs. MHII media was due to inhibition of drug's activity by MHII or enhancement of its activity by RPMI, we mixed RPMI and MHII media in equal parts together and used this media to test the MIC. The MIC of RBT was 8 μg/mL in the hybrid media, similar to the rich media and much higher than the nutrient-limited media (Table 1). Thus, the rich MHII media antagonized the hyper-activity of RBT.

To identify the inhibitory agent(s) in rich media, we separated MHII fractions and tested each by adding them to RPMI and repeating the MIC assay (Table 1). We were unable to remove the antagonizing component in rich media by proteinase K or sodium periodate

treatments which suggested that the antagonizing factor was not a polypeptide or carbohydrate species (Table 1). Interestingly, we did identify that free, hydrophobic amino acids, alone and in combination, could reduce RBT activity in nutrient-limited media (Table 1).

We also modulated iron levels in the media since RPMI is highly iron-depleted compared to MHII [24,25]. We found that increasing the iron content in RPMI antagonized RBT and increased the MIC. In contrast, lowering the iron content in MHII media increased the potency of RBT and lowered the MIC (Fig. 2A, Extended Data Fig. 2).

We hypothesized that inhibition of RBT's hyper-activity was related to reduction in uptake of the antibiotic into the bacterial cell in rich but not nutrient-limited media. We therefore sought to measure the accumulation of RBT in the bacteria by LC/MS (Fig. 2B). CFU density and RNA transcription were inversely correlated with intracellular drug accumulation, consistent with the known mechanism of rifamycin antibacterial effect (inhibition of RNA transcription). We found that adding amino acids to nutrient-limited media reduced RBT entry into the bacterial cell, to levels similar to those seen in rich media, enabling a greater number of surviving bacteria and increased transcription (Fig. 2B-D).

Since free, hydrophobic amino acids were mediating the antagonism of RBT activity in RPMI, we hypothesized that RBT, and not RIF, was entering the bacterial cell through amino acid transporters. We evaluated single gene transposon-disrupted mutants of known amino acid transporters, including *apoP, tryP, hisM, mtr, hisP,* and *hisJ,* but we did not observe a difference in MIC (Extended Data Fig. 3).

Therefore, to identify the gene(s) responsible for the hypersensitivity phenotype in the RPMI media, we selected for HUMC1 spontaneous mutants that lost their hyper-sensitivity phenotype to RBT. We passaged bacteria on RPMI agar plates supplemented with 1 μg/mL RBT, and then sequenced genomes of the resulting mutants (Supplementary Data File 2). To determine the effect of the most commonly identified gene mutations, individual transposon mutants were obtained from the *Acinetobacter baumannii* mutant library[26] and RBT MICs were determined (Extended Data Fig. 4). Only *fhuE* disrupted mutants displayed a shift of the RBT MIC from 0.05 μg/mL of the parent strain to 3.13 μg/mL of the mutant (Extended Data Fig. 4). A second, independent mutant selection experiment also identified resistant mutants with *fhuE* mutations (Extended Data Fig. 5). Defined *fhuE* mutants were also generated to confirm the observed phenotype (Extended Data Fig. 6).

FhuE has been previously described as an iron-regulated, outer membrane protein transporter that is involved with iron acquisition in bacteria.[27] We found that *fhuE* expression was upregulated in low iron conditions (RPMI and iron-depleted MHII), and expression was downregulated in high iron conditions (RPMI + iron citrate, and MHII) (Fig. 2E). The addition of hydrophobic amino acids did not alter *fhuE* expression. The lack of change of expression of *fhuE* but inhibition of uptake of RBT mediated by amino acids even in low iron conditions (in which *fhuE* is expressed) indicated that amino acids worked by competitive inhibition of RBT uptake via the expressed transporter, rather than by altering

its expression. Thus RBT hyperactivity requires both low iron and low free amino acid conditions.

Of 43 *A. baumannii* clinical isolates tested *in vitro,* 65% had a hyper-sensitive phenotype in nutrient-limited media, while the remainder had MICs similar between nutrient-limited and rich media (i.e., the rifabutin remained active, still exhibiting microbial killing at concentrations achievable *in vivo*, even for non-hypersusceptible strains). We sought to determine if differences in the amino acid sequences of the FhuE protein in *A. baumannii* accounted for these susceptibility differences. Using a panel of *A. baumannii* clinical isolates from the CDC and FDA Antibiotic Resistance Isolate Bank, we created a phylogenetic clustering based on the amino acid sequence of the FhuE protein. The outer ring was represented predominantly by isolates that were hypersensitive (MIC < 0.05 μg/mL) to RBT in RPMI. The inner ring was made up of isolates that were found to have a higher MIC (>3.13 μg/mL) to RBT in RPMI (Extended Data Fig. 7). Hence, FhuE amino acid sequences correlated with the hyper-sensitive phenotype.

To confirm that expression of the *fhuE* isoform from HUMC1 ($fhuE^{Humc1}$) was sufficient to reproduce the RBT hypersensitivity phenotype, we created a $fhuE^{Humc1}$ overexpression construct under the control of an inducible promoter in a strain disrupted of *fhuE* or its wild-type parent. We showed that overexpression of $fhuE^{Humc1}$ resulted in increased ATCC17978 sensitivity to RBT and was able to complement the Δ*fhuE* mutant (Fig 2F, Extended Data Fig. 8). Overexpression of $fhuE^{Humc1}$ in LAC-4, a strain that encodes a different *fhuE* isoform that clusters with the non-hypersensitive group, also increased sensitivity to RBT (Fig 2C). Thus, $fhuE^{Humc1}$ expression was sufficient to recapitulate the hyper-sensitivity phenotype.

The discrepancy between RBT activity against *A. baumannii* in nutrient-limited RPMI vs. rich MHII media led to a critical question: which media was better predictive of *in vivo* efficacy of RBT? In an immunocompromised neutropenic lung infection model, we observed a significantly greater reduction in CFUs in mice infected with *A. baumannii* UNT091-1 (wild-type) and treated with RBT as compared to RIF (Fig 3A). Furthermore, the effect of RBT was blunted in mice infected with the UNT091-1::Δ*fhuE* strain (Fig 3A) supporting the role of *fhuE* as mediating RBT sensitivity both *in vitro* and *in vivo*.

We next tested the RBT efficacy in a normal, immunocompetent *A. baumannii* pneumonia infection model. Mice were infected with *A. baumannii* HUMC1 and treated with 10 mg/kg/day RIF or RBT. At 24 hours, RBT-treated mice had a 7-log reduction in the median CFUs in the blood as compared to RIF-treated mice. At the 10 mg/kg dose, RBT also improved survival vs. RIF, although RIF was partially effective vs. placebo at that dose. (Fig. 3B).

We then lowered the dose of both drugs to 5 mg/kg/daily to determine if RBT enhanced potency would be unmasked. At the lower dose, RBT-treated mice had significantly reduced lung CFUs and markedly improved survival vs. RIF (Fig. 3C). No difference was observed between the RIF and PBS control group.

Next, we tested if RBT was more effective than RIF in an immunocompetent intravenous model of infection. Mice were infected IV with HUMC1 and treated with 10 mg/kg/day RIF or RBT. RBT-treated mice had significantly lower CFUs and improved survival (Fig. 3D). Lastly, we found that RBT was fully protective when dosed at 300x lower than a RIF dose that was minimally protective (Fig. 3E). Similarly, we also observed that RBT was protective in a *G. mellonella* infection model at significantly lower doses as compared to RIF (Extended Data Fig. 9A).

However, there was no difference in efficacy of RBT or RIF in mice or in *G. mellonella* infection models against *A. baumannii* LAC-4, a strain which has a distinct FhuE isoform and no difference in RBT/RIF MICs in nutrient-depleted media (Fig. 3F, Extended Data Fig 9B, C).

RBT would likely be used clinically in combination with a second antibiotic, a practice that is standard with the use of rifamycin antibiotics. We measured the spontaneous frequency of resistance emergence to RBT *in vitro* by culture *A. baumannii* HUMC1 overnight in MHII or RPMI and plating bacteria on agar plates supplemented with RBT alone, colistin (COL) alone, or RBT + COL. We were unable to select for any spontaneous mutants in the double selective plates (Fig 4 A, B). Additionally, we found that RBT and COL interacted synergistically *in vitro* (Extended Data Fig. 10). We determined the spontaneous frequency of resistance emergence to RBT *in vivo* by infecting mice and then harvesting blood and kidneys at 16.5 hours post infection and then plating samples on agar plates supplemented with RIF alone or RBT alone. The frequency of spontaneous RBT resistance emergence was <1.7E-9 and <3.7E-8 CFUs *in vivo* (Table 2). These values were about 10-fold less as compared to the frequency of spontaneous RIF resistance emergence which were 8.4E-8 and 1.2E-7 CFUs in the blood and kidneys, respectively. Furthermore, we found that the treatment combination of RBT + COL was syngergistic *in vitro*, even with the less sensitive Δ*fhuE* mutant (Extended Data Fig. 10), and that the combination of RBT + COL is more effective *in vivo* (Fig 4C).

Thus, these collective experiments confirmed that RBT has an excellent activity in vivo and is more potent when compared to RIF, and that *in vitro* MIC results in nutrient-limited media better predicted *in vivo* efficacy than *in vitro* MIC results in rich media. The superiority of RBT over RIF is highly significant due to a recent, randomized, controlled clinical trial that found a non-significant trend to improved clinical cure, with a significant improvement in microbiological eradication when adding rifampin to colistin for treatment of XDR *A. baumannii* infections [28]. Given that RIF had some effect clinically, and that RBT appears far more potent and effective in pre-clinical models, we believe that the addition of adjunct RBT, as compared to RIF, could serve as a critically needed therapeutic option for patients with infections caused by XDR *A. baumannii,* potentially resulting in superior survival compared to the current standard of care. Thus, studies with RBT are underway to evaluate clinical utility of this promising drug for the treatment of *A. baumannii* infections where there are currently limited treatment options.

Finally, high throughput screens of small molecules have been a standard practice for the pharmaceutical industry for decades. These libraries, which may contain millions of

compounds, have been screened many times; however, new screens of the same library rarely identify novel compounds [7,29]. Our results demonstrate that using more physiologically relevant, nutrient-limited media has the potential to identify many additional treatments for antibiotic-resistant bacterial infections which have been missed to date due to screens of these large libraries based on rich culture media [7,30,31]. Thus, repeat screening of these large libraries in nutrient-limited media may offer a promising, critically-needed approach to identifying antimicrobial agents with which to combat the crisis of antibiotic-resistant infections.

Materials and Methods

Ethics statement

All animal work was conducted following approval by the Institutional Animal Care and Use Committee (IACUC protocol 20882) at the University of Southern California, in compliance with the recommendations in the Guide for the Care and Use of Laboratory Animals of the National Institutes of Health. Infected mice develop weight loss, ruffled fur, poor appetite, decreased ambulation, huddling behavior, and low body temperature. Mice that display huddling behavior and are poorly mobile will be weighed 1x daily. Weight loss of greater than 15% body weight will trigger euthanasia. Mice were monitored at least twice daily for seven days. Soft bedding and other enrichment devices were provided as recommended by the vet staff. Nutritional supplements, such as the hydrogel packs were provided as needed.

Source of bacterial isolates

The complete list of bacterial isolates tested is listed in Data File 1. Strains were obtained from the CDC Antimicrobial Resistance Isolate Bank, the She lab, the Spellberg lab, and BioVersys.

Bacteria Culture

Working solutions of bacteria were prepared using frozen stocks of *Acinetobacter baumannii* strains as previously published,[16] or by inoculating a fresh overnight culture in Tryptic Soy Broth (TSB) and incubating at 37°C/200 rpm. The overnight culture was diluted 1:100 and then subcultured in MHII at 37°C/200 rpm until the culture reached an OD_{600} of 0.5. For some assays, bacteria were also subcultured in Roswell Park Memorial Institute (RPMI) 1640 Medium (Gibco, 11875119).

High Throughput Compound Screening

Compounds from the 10 mM ReFRAME library stock [14] were acoustically transferred using the Echo 555 Liquid Handler (Labcyte Inc.) at 20 μM final assay concentration into 1536-well plates. Log-phase growth *A. baumannii* HUMC1 was diluted in assay media (MHII or RPMI with and without 50% normal mouse serum) and dispensed into assay plates using the MultiFlo FX Multi-Mode Dispenser (BioTek). Bacterial viability was assessed 24 hours later using the BacTiter-Glo Microbial Cell Viability Assay (Promega) and the PHERAstar microplate reader (BMG Labtech). Positive controls included 10 μM colistin and doxycycline. Assay was normalized to neutral and positive controls and putative hits were

selected based on 50% reduction in viability. Putative hits were re-tested in single point triplicate and upon reconfirmation were further tested in an 8-point 1:3 dose response and counter-screened against mammalian HepG2 and HEK293T cell lines using a 72-hour CellTiter-Glo Luminescent Cell Viability Assay (Promega). For the mammalian cytotoxicity counter screen 40 μM puromycin (Sigma) was used as the positive control and data was normalized as for the primary assay. All data were uploaded to and analyzed in Genedata Screener, Version 13.0.1-Standard. Replicate data were analyzed using median condensing. Dose response curves were fitted with the four parameter Hill Equation.

Antibiotic Preparation—RIF (Sigma, R3501-1G) and RBT (Sigma, R3530-25MG) were dissolved in Dimethyl sulfoxide (DMSO). The working solution of antibiotic was prepared 2X of the desired starting well final drug concentration. The antibiotic working solution dilutions were prepared in the respective media used for the MIC, MHII or RPMI.

MIC Protocol

Unless otherwise indicated, the standard broth microdilution method was used to determine MICs.[5] The medium used for the minimum inhibitory concentration (MIC) assays performed in this study was either MHII or RPMI 1640.

Briefly, 100 μL of media, RPMI or MHII, was added to the wells in columns 2-10. Column 11 served as a positive growth control and contained only bacteria and media. Column 12 served as the negative control and contained only culture media without bacteria. Next, 200 μl of a 2X rifabutin or rifampin working solution was added to the wells in column 1. Two-fold serial dilutions of the antibiotic were performed through column 10. Next, 100 μl of a 1×10^6 CFU/mL working solution of bacteria was added to each of the wells in columns 1-11. The inoculum concentration was confirmed by plating serial dilutions on TSA plates. MICs plates were incubated at 35±2 °C without shaking and results were recorded at 24 hours.

To test the effect of the individual components of MHII, MHII fractions (size separation, acetonitrile extracted, proteinase K digested, or sodium periodate oxidized), 10 μL of the purified fraction was added to the appropriate wells.

As indicated, amino acids were used to supplement the media for MIC testing. Mixed amino acids were tested by adding 10 μL of Gibco® MEM Amino Acids Solution (Thermo Scientific, #11130051) and Gibco® MEM Non-Essential Amino Acids (Thermo Scientific, #11140050) to each well in the MIC assay. Additionally, the effect of individual amino acids on the MIC was tested by the addition of purified amino acids at the same concentration contained in the Gibco mixed amino acid solutions listed above. Amino acids were prepared fresh and filter sterilized solutions prior to use.

For some MICs, efflux pump inhibitors were added to the media. Efflux pump inhibitor MICs were performed to identify subinhibitory concentrations of the efflux pump inhibitors. The final concentration of inhibitors used were as follows: verapamil (50 μg/mL), thioridazine (8 μg/mL), and CCCP (2 μg/mL).

For MICs involving the *fhuE*^{Humc1} overexpression strains, the respective stains were cultured overnight and subcultured in low salt LB supplemented with 250 μg/mL zeocin at 37 °C/200 rpm to maintain the overexpression plasmid. MIC assays were done in MHII or RPMI media supplemented with 20 μg/ml of zeocin to maintain the plasmid. Expression of *fhuE* was induced by the addition of arabinose at the final concentrations of 8%, 4%, 1%, or no arabinose as a control.

Fractional inhibitory concentration index(FICI)—Drug -drug interaction between rifabutin or rifampin and colistin in MHII The drug-drug interaction were evaluated by calculating the fractional inhibitory concentration index(FICI). FICI=FIC_A+ FIC_B=(C_A/MIC_A)+(C_B/MIC_B), in which C_A and C_B are drug concentration of drug A and drug B in combination and MIC_A and MIC_B are the MIC of drug A and drug B alone. Synergy was defined as FICI≤0.5, no interaction was defined as FICI >0.5–4.0 and antagonism was defined as FICI >4.0.

Fractionation of MHII:

Size fractionation—10X MHII was used for the fractionation to maximize the concentration of the MHII components. The media was filtered through a 0.22 μM filter and then the media was run through 10 and 30 kDa molecular weight cut-off (MWCO) centrifugal filtration columns at 12,000 g for 20 minutes. The >30 kDa fraction was collected and reserved for experimentation. The flow through was collected and transferred to a 10 kDa MWCO column. The centrifugation step was repeated as previously stated. The <10 kDa flow through was collected from this column. The 10<X<30 kDa fraction was collected as well.

Acetonitrile Extraction—The organic and inorganic layers were separated with a liquid-liquid extraction by mixing the purified MHII fraction 1:1 with 100% acetonitrile. The sample was vortexed thoroughly and centrifuged at maximum speed for 10 minutes. The aqueous and organic layers were transferred to clean microcentrifuge tubes. To ensure the removal of any residual acetonitrile, the extracted MHII sample was dried using a SpeedVac and then resuspended in the original volume using sterile molecular grade H_2O.

Proteinase K Digestion—30 μl of proteinase K (Invitrogen, #46-7603) was added to 1 mL of the MHII <10 kDa fraction (organic extract or non-extracted as a control). The media was incubated at 65°C for 1 hour. To inactivate the proteinase K, the sample was then incubated at 80°C for 15 minutes.

Sodium Periodate Oxidation—Sodium periodate oxidation was done as previously described.[32] Briefly, to oxidize the carbohydrates in the organic layer of the medium, sodium periodate (NaIO4) was added to the <10 fraction at a final concentration of 10 mM. The sample was incubated at room temperature for 30 minutes. Following incubation, the sodium periodate was quenched using 0.1 mL of 50% glycerol for every 1 mL of reaction. The sample was incubated at room temperature for 1 hour before downstream application.

Time Kill Assay—Time kill assays were performed in a 96-well U-bottom plate using the same plate set up as the MIC assay. We measured viable cell counts at 1, 8, and 24 hours. At each time point, the contents of an individual well were collected and CFUs were determined by plating serial dilutions on TSA plates and incubating overnight at 37°C.

As a control, the remaining wells of the 96-well plate were returned to the incubator after each sample collection and an MIC was determined as described above.

Mass Spectrophotometry—Extractions and measurements were done as previously described [33,34]. Log-phase *A. baumannii* culture was incubated 0.79 or 0.38 μg/mL RBT in the presence or absence of amino acid mixture at 37 °C. Bacteria were harvested 0, 1, 8, and 24 hours and CFUs were determined by plating serial dilutions on agar media. The cell free supernatant was collected by filtration through a 0.22 μm filter. RBT were extracted by adding LC-MS grade acetonitrile:methanol:water (40:40:20) solution that was precooled to − 40 °C. Liquid chromatography mass spectrometry (LC-MS) differentiation and detection of RBT was performed using a Cogent Diamond Hydride Type C column (Microsolve Technologies) with an Agilent Accurate Mass 6230 TOF coupled with an Agilent 1290 Liquid Chromatography system as previously published.[33,35] An isocratic pump was used for continuous infusion of a reference mass solution to allow mass axis calibration. Detected RBT ion was validated based on unique accurate mass-retention time identifiers for masses. RBT level was analyzed using Agilent Qualitative Analysis B.08.00 (Agilent Technologies) with a mass tolerance of <0.005 Da. The intracellular RBT was calculated as the $[RBT]_{\text{drug only control}} - [RBT]_{\text{filtrate}}$. 3 biological replicates were tested per group.

Selection of spontaneous RBT-resistant mutants and WGS:

The RBT hypersensitive strain HUMC1 was cultured overnight in 50 mL of RPMI. Bacteria were plated on RPMI agar plates supplemented with 1μg/mL of RBT. Individual colonies were selected and then counter screened in RPMI agar plates supplemented with 25 μg/mL RBT.

Colonies that grew on the RPMI agar plates supplemented with 1 μg/mL, but not the 25 μg/mL RBT, were processed for whole genome sequencing. Sequencing libraries for the selected mutants and parent strain were prepared at the USC Molecular Genomics Core. Libraries were simultaneously prepared from extracted genomic DNA using the Illumina Nextera XT library prep kit according to the manufacturer's protocol (Cat#FC-131-1024, Illumina). Prepared libraries were sequenced on the Illumina Miseq V2 at 2x150 cycles. Assembled reads were aligned to the previously published *A. baumannii* HUMC1 sequence (NCBI Reference Sequence: NZ_LQRQ01000007.1). The FASTQ files were uploaded to PartekFlow® software, version 6.0 (Partek, Inc., St. Louis, MO) on a Linux based High Performance Computing system at Pennsylvania State University College of Medicine, adapter-trimmed, and remapped to HUMC1 reference sequence(NZ_LQRQ01000007.1) using alignment algorithm (BWA-MEM) with a few modifications (mismatch penalty 4, gap open penalty 6, clipping penalty 5, and alignment score cutoff 30) for short read mapping. After alignment, annotated variants were saved.

FhuE phylogenetic tree—Maximum-Likelihood phylogenetic tree of 43 fhuE aminoacid sequences, constructed using the CLC Genomics Workbench 12 (Qiagen) software. Nucleotide sequences were generated by assembling SRA reads of the 41 clinical isolates from the CDC and FDA Antibiotic Resistance Isolate Bank and aligning to the HUMC1 or LAC4 fhuE template. Numbers at the base of nodes correspond to bootstrap (10.000) probability >90%. The scale indicates the number of amino acid substitutions per site.

***fhuE*^{Humc1} overexpression construct—**The open reading frame of the fhuE gene was cloned into the pVRL2Z plasmid under the control of the arabinose indcubible promoter. HUMC1 genomic DNA and pVRL2Z plasmid DNA were extracted using the Quick-DNA Fungal/Bacterial Kits (Zymo, #D6005) and the GeneJET Plasmid Miniprep Kit (Thermo Fisher, #K0502), respectively. The open reading frame of the *fhuE* gene from HUMC1 was cloned by PCR using oligonucleotide primers (5'-taa gca GAA TTC GCA TCG AGG GTT GCAT TTC C-3' / 5'-taa gca GCG GCC GCT CTA CTT CAC CCT TGC GGC T-3') and purified using PureLink® PCR Purification Kit (Thermo Fisher Scientific, #K310001). The Q5® High-Fidelity 2X Master Mix (NEB, M0492S) was used for all cloning related PCRs. The vector and insert were both digested with NotI/EcoRI (NEB, #R0189S/NEB, #R0101S), digested products were purified, and the vector/insert were ligated using T4 ligase (NEB, #M0202S).

Transformation of *A. baumannii* AB5674, ATCC 17978, and LAC-4 was performed by electroporation using freshly prepared competent cells. Transformants were selected on low salt LB agar supplemented with 250 μg/ml of zeocin. Transformants were confirmed by reisolating the plasmid by miniprep, digestion of the plasmid DNA using NotI/EcoRI, and visualizing the digested products on an agarose gel.

Electrocompetent cells were prepared as by subculturing bacteria to log-phase growth in TSB at 37°C/200 rpm/2.5 hrs. Bacteria were collected by centrifugation and the cell pellet was washed in 1 mL of ice-cold 10% glycerol by pipetting up and down. Cells were collected by centrifugation at 16,000 rcf/5 min/4°C. Bacteria were washed 5X and resuspended in 300 μl of 10% glycerol. 100 μL of electrocompetent cells were used for each transformation.

RNA extraction—Bacteria were cultured overnight in different media conditions (Fig. 2B) at 37 °C/200 rpm. Bacteria were subcultured to log-phase at 37°C/200 rpm/3 hrs and RNA was extracted with the RiboPure™ RNA Purification Kit per manufacturer protocol (Thermo Fisher Scientific, #AM1925).

Quantitative fhuE gene expression—cDNA was synthesized by using LunaScript™ RT SuperMix Kit (NEB, #E3010L) after normalizing RNA template. Targets were amplified as using the Luna® Universal qPCR Master Mix (NEB, #M3003S) per manufacturer protocol and the following primers. HUMC1 fhuE: 5'-GGC GTT AGA GAA ACA CCG GA-3' / 5'-GGC GCA CTG GGA TAA TGA GA-3'; rpoD: 5'-GCG TGA AAT GGG TAC AGT AGA A-3'/ 5'-TTG GCC AGT AAG CGA TTG AG-3'; LAC4 fhuE: 5'- CCC ATT GCG AAC CAT TAG CG-3' /5'-ACA CAA GAT GGG CGA GTA CG-3'. Expression of *fhuE* was normalized to the housekeeping gene *rpoD* using the ΔΔCT method.

fhuE* gene deletion—fhuE* was knocked out using a two-step recombination method previously described [36]. DNA regions (700 bp) flanking *fhuE* were PCR amplified using the following primers. fhuE-up: 5'-AGA ATT GAG GCC TCT CGA GGA ATT CTT GAT GCC ATG TAC TCG C-3' / 5'-CCA TAA AAA GGT TGG CAT AAC AAA TCG C-3'; fhuE-down: 5'-TTA TGC CAA CCT TTT TAT GGT GCC CCA G-3' / 5'-CCT GCA GGC TCT AGA CAT CGA GGG TTG CAT TTC-3'. The fhuE up- and downstream fragment were cloned in the knockout platform pVT77 previously digested with EcoRI/XbaI using NEBuilder HiFi DNA assembly (NEB). The cloned *fhuE* knockout plasmid was conjugated in *A. baumannii* and genomic plasmid integration was selected on LB agar plates containing 100 μg/ml sodium tellurite. Obtained clones were transferred on LB agar plates containing 1 mM isopropyl-β-D-1-thiogalactopyranoside and 200 μg/ml 3'-azido-3'-deoxythymidine to select for plasmid removal from the genome. Scarless deletion of *fhuE* was screened with primers 5'-TAC TTC ACC CTT GCG GCT AC-3' / 5'-AAA GAT ACG ACC AAC CGC CC-3' and confirmed by DNA sequencing (Microsynth AG, Balgach, Switzerland).

GFP expression—Transformation of *A. baumannii* ATCC 17978 was performed by electroporation using freshly prepared competent cells. Transformants were selected on TSA agar supplemented with 10 μg/ml of gentamicin (Sigma, #G1272). Transformants were confirmed by GFP expression using a fluorescent plate reader.

Transformants were then subcultured in RPMI supplemented with 10 μg/ml of gentamicin with 4% arabinose. 1×10^5 CFU bacteria and the appropriate concentration of RBT were added to RPMI supplemented with 10 μg/ml gentamicin and 4% arabinose, up to the total volume of 200μl. 10 μl of AA was added in appropriate samples as well. GFP expression was measured using flow cytometry analysis every 30mins.

G. mellonella* infection model—Galleria mellonella* larvae (10 per group) were infected with logarithmic phase growing (OD_{600} = 0.5) bacteria resuspended in PBS to reach the specified cfu/larvae with a 10 μl injection in the right second proleg. The infected larvae were subsequently treated with rifabutin or rifampicin 1 hour after infection with a 10 ul injection of the specified antibiotic dose in the left second proleg. The injected larvae were incubated at 37 °C in 90-mm plastic Petri dishes and monitored for their survival for 72 h. Larvae were considered dead when they did not move in response to stimulus with a pipette tip.

***In Vitro* Mutant Selection—**Spontaneous rifabutin and colistin resistant mutants were selected by high inoculum plating on selective agar plates supplemented with 8 μg/mL of rifabutin, 16 μg/mL of colistin or the combination of both antibiotics. Overnight cultures of *A. baumannii* HUMC1 were grown in 20 ml MHII or RPMI at 37°C / 200 rpm. For bacteria cultured in MHII, 100 μL of culture was plated directly on selective plates to enumerate the antibiotic-resistant population and serial dilutions were plated on non-selective plates to enumerate the total population. Because the bacteria grow to a lower density in RPMI, the bacteria were first concentrated by 10x by centrifugation prior to plating on non-selective and selective agar plates as described above. All experiments were done in triplicate.

Mouse Studies—Mice were randomly assigned to treatment groups and treatment groups were not blinded.

Intravenous (IV) infection—*A. baumannii* HUMC1 frozen stock was prepared as described in previous work.[16] Frozen stocks of HUMC1 were thawed and diluted in PBS to adjust the bacterial density as needed for infection. Male C3HeB/FeJ mice, 8 to 12 weeks old, were infected with $2x10^7$ CFUs via tail vein injection and the inoculum bacterial density was confirmed by plating serial dilutions on TSA plates and incubating overnight at 37°C.

Oral aspiration (OA) infection—Single colonies of *A. baumannii* HUMC1 grown on TSA were used to inoculated TSB and bacteria were cultured overnight at 37°C / 200 rpm. The following day, the bacteria was subcultured by diluting the overnight 1:100 in fresh TSB and cultured for 3hrs at 37°C / 200rpm. The subculture was washed with PBS three times and adjust to optical density (OD_{600}) equal to 0.5. The inoculum was concentrated to $2x10^9$ CFUs/ml and 9 to 10 weeks old male C3HeB/FeJ mouse is infected with 50 μL ($1x10^8$ CFUs) of inoculum via oral aspiration. The inoculum CFUs was confirmed by plating on TSA plates and incubating overnight at 37°C.

Neutropenic pneumonia infection—Female CD-1 mice were made neutropenic by the administration of 150 & 100 mg/kg of cyclophosphamide, intraperitoneally (IP), at 4 and 1 day prior to infection. Frozen stock of *A. baumannii* BioVersys UNT091-1 and UNT091-1::ΔfhuE were plated on TSA and incubated overnight (ON) at 37°C. The plate growth was suspended into TSB to 1.0e+09 CFU/mL (OD 1 @ 600 nm), and then 10-fold serial diluted in fresh TSB and this log10 dilution was used as the infecting inoculum. The infecting inoculum was approx. 6-7 $\log_{10}$ CFU/animal. Additionally, the OD adjusted plate suspension was 10-fold serially diluted and spot plated onto BHI/charcoal plates to determine input CFU.

Mice were anesthetized by IP injection 0.2 ml of a Ketamine HCL (40 mg/kg b.w.) + Xylazine (6 mg/kg b.w.) mixture. Anesthetized mice were intranasally (IN) inoculated with 0.05 ml of the designated inoculum. For IN inoculation, drops were placed onto the eternal nares and waited for inhalation. After inoculation, each mouse was placed back into their cage with heat pads for recovery. Plate counts were performed to confirm the exact CFU input for each strain (targeting 6.5 $\log_{10}$ CFU/mouse).

Mice were euthanized by CO_2 inhalation at 26 hrs post-infection, lungs aseptically removed, placed in cold PBS, homogenized, serially diluted and spot plated on BHI + charcoal for the determination of bacterial lung titers ($\log_{10}$ CFU/lung). Colony counts were performed on the agar plates. The number of colonies was converted to CFU/lung by multiplying the number of colonies by the volume of the lung homogenate spotted and the dilution at which the colonies were counted (5-50 colonies/spot). All count data were transformed into $\log_{10}$ CFU/lung for calculation of means and standard deviations. The limit of detection was $\text{Log}_{10} = 2.35$

Mice were inoculated intranasally with equivalent titers (6.75 and 6.90 $\log_{10}$ CFU) of each of the two A. baumannii strains and the treatment (single IV dose) with rifabutin and rifampicin was administered at 2-hour post-infection.

Antibiotic treatments—RIF (Sigma, R3501-1G) and RBT (Sigma, R3530-25MG) were dissolved in Dimethyl sulfoxide (DMSO). The working solution of antibiotics are prepared fresh daily. The appropriate concentration of antibiotic working solution was prepared in PBS with 10% DMSO and administered by oral gavage. The control mice received the same volume of PBS with 10% DMSO without drug. RIF, RBT, and the control were administered once a day for three days starting the day of infection.

Blood CFUs—50 - 100 μL of blood was collected by tail nick at the indicated time points post OA or IV infection. Blood samples were serially diluted in PBS and plated on TSA plates. Agar plates were incubated overnight at 37°C and CFUs were counted the next day.

Lung CFUs—At 18 hrs post infection, lungs were harvested, weighed, and homogenized in sterile PBS. Lung homogenates were serially diluted in PBS and plated on TSA plates. The plates are incubated overnight at 37°C and CFUs were counted the next day.

Mutant Selection—Male C3HeB/FeJ mice were infected with 2.7 x 10^7 CFUs of *A. baumannii* HUMC1. Mice did not receive RIF or RBT treatments. Blood and kidneys were collected 16.5 hrs post infection and samples were plated on TSA or RPMI agar plates alone or supplemented with 8 μg/mL RIF or RBT.

Statistics—Bacterial burden was compared using the Mann Whitney test. Time to death was compared using the Log Rank test. P values < 0.05 were considered significant.

Data Availability

Screening data are available on ReFRAMEdb.org. Genome sequencing data are available at NCBI Accession PRJNA629056. Source data for the figures are provided with the paper.

Extended Data

Species	Strains	Rifabutin MIC (μg/mL)
P. aeruginosa	PAO1	8
	ATCC-27853	8
K. pneumonieae	ATCC-43816	16
	ATCC-27736	16
E. coli	ATCC-25922	4
	ATCC: BAA-2471™	8

Extended Data Fig. 1. MIC of rifabutin in RPMI + 10% FCS on non-*A. baumannii* Gram-negative ESKAPE species.

Strain	Iron (μM) in RPMI + 10% FCS	MIC (μg/mL)
HUMC1	0	0.001
	0.1	0.002
	0.5	0.004
	1	0.004
	5	0.016
	10	0.016
	50	1
	100	4

Extended Data Fig. 2. MIC of rifabutin in RPMI + 10% FCS supplemented with increasing amount of ammonium iron(III) citrate.

Strain	Disrupted Gene	RBT (μg/mL) MHII	RPMI
HUMC1		6.25	0.05
AB5075-UW		6.25	0.05
AB00188	aroP	3.13	0.05
AB00190	aroP	6.25	0.05
AB03015	aroP	6.25	0.05
AB02204	aroP	6.25	0.05
AB09979	aroP	0.78	0.05
AB09980	tryP	3.13	0.05
AB00215	tryP	6.25	0.05
AB03612	hisM	3.13	0.05
AB03616	hisM	6.25	0.05
AB03618	hisM	6.25	0.05
AB06383	hisJ	6.25	0.05
AB07813	mtr	25	0.05
AB02205	aroP	3.13	0.05
AB07354	aroP	6.25	0.05
AB07356	aroP	1.56	0.05
AB09982	tryP	6.25	0.05
AB00216	tryP	1.56	0.05
AB06392	hisP	0.78	0.05
AB06386	hisP	0.78	0.05
AB06105	aroP	3.13	0.05
AB03608	hisJ	3.13	0.05

Extended Data Fig. 3- Rifabutin MICs against *A. baumannii* AB5075 transposon disruption mutants.

Mutants were deficient in amino acid transport genes. MIC assay was done in both MHII and RPMI media. AB5075-UW is the parent strain for the transposon mutants.

Strain	AB locus	Disrupted gene	MHII	RPMI
AB05671	ABUW_2165	TonB-dependent siderophore receptor (fhuE)	3.13	3.13
AB05672	ABUW_2165		6.25	3.13
AB05673	ABUW_2165		3.13	3.13
AB05674	ABUW_2165		3.13	1.56
AB10057	ABUW_3811	DID	3.13	0.05
AB10058	ABUW_3811		3.13	0.05
AB06731	ABUW_2557	hypothetical protein	3.13	0.05
AB06732	ABUW_2557		6.25	0.05
AB06076	ABUW_2318	cytosine permease	3.13	0.05
AB06077	ABUW_2318		1.56	0.05
AB05837	ABUW_2228	TonB-dependent receptor	3.13	0.05
AB05838	ABUW_2228		3.13	0.05
AB05361	ABUW_2062	phospholipase D family protein	1.56	0.05
AB05362	ABUW_2062		1.56	0.05
AB07566	ABUW_2893	hypothetical protein	0.78	0.05
AB07567	ABUW_2893		0.78	0.05
AB02034	ABUW_0745	hypothetical protein	0.78	0.05
AB02035	ABUW_0745		1.56	0.05
AB09112	ABUW_3470	Zn-dependent hydrolase	0.78	0.05
AB09114	ABUW_3470		0.78	0.05
AB01188	ABUW_0449	hypothetical protein	1.56	0.05
AB01192	ABUW_0449		1.56	0.05
AB04576	ABUW_1741	outer membrane protein assembly factor BamA	1.56	0.05
AB05479	ABUW_2100	LysR family transcriptional regulator	3.13	0.05
AB05480	ABUW_2100		1.56	0.05
AB05756	ABUW_2194	acyl-CoA dehydrogenase	1.56	0.05
AB05757	ABUW_2194		6.25	0.05
AB06047	ABUW_2307	biotin synthase	0.05	0.05
AB06049	ABUW_2307		0.05	0.05
AB06089	ABUW_2322	integrase	3.13	0.05
AB06091	ABUW_2322		6.25	0.05
AB05348	ABUW_2057	alcohol dehydrogenase	1.56	0.05
AB05089	ABUW_1933	NADP-dependent fatty aldehyde dehydrogenase	1.56	0.05
AB04593	ABUW_1750	HAD-superfamily hydrolase	3.13	0.05
AB04594	ABUW_1750		3.13	0.05
AB02891	ABUW_1069	NADH dehydrogenase	3.13	0.05
AB02892	ABUW_1069		6.25	0.05
AB06694	ABUW_2539	IS4 family transposase	3.13	0.05
AB06695	ABUW_2539		3.13	0.05
AB01494	ABUW_0559	putative phage-related membrane protein	3.13	0.05
AB01495	ABUW_0559		6.25	0.05
AB06821	ABUW_2586	allophanate hydrolase	3.13	0.05
AB06822	ABUW_2586		3.13	0.05
AB04749	ABUW_1817	putative peroxidase(alpha/beta hydrolase)	3.13	0.05

Extended Data Fig. 4 - Rifabutin MICs against *A. baumannii* AB5075 transposon disruption mutants.

MIC assay was done by culturing the bacteria in either MHII or RPMI media.

Collection day	Serial passage medium	Antibiotic pressure	MIC (μg/mL)		WGS mutations
			Rifabutin in RPMI + 10% FCS	Rifampicin in CA-MHB	
HUMC1 ancestor strain			0.004	4	Reference genome
Day 14 (96 well plate serial passage)	RPMI + 10% FCS	RBT	4	4	- transposon insertion in AWC45_RS10145 (TonB-dependent siderophore receptor), Arg149fs* - transposon insertion in AWC45_RS12960 (TonB-dependent siderophore receptor), Asp689fs*
	RPMI + 10% FCS	RIF	0.004	8	ND
	CA-MHB	RBT	0.004	4	ND
	CA-MHB	RIF	0.008	16	ND
Day 3 (tube serial passage)	RPMI + 10% FCS	RBT	4	4	- insertion mutation in AWC45_RS10145 (TonB-dependent siderophore receptor), Ile364fs*
	RPMI + 10% FCS	RIF	0.008	> 32	ND
	CA-MHB	RBT	> 32	> 32	- transposon insertion in AWC45_RS10145 (TonB-dependent siderophore receptor), Ile433fs* - RpoB D525N mutation
	CA-MHB	RIF	0.12	> 32	- RpoB S521F mutation

Extended Data Fig. 5. MIC of rifabutin and rifampicin on HUMC1 and the serial passaged mutants, and WGS of mutants with increased rifabutin MIC.

Strains	MIC (μg/mL)	
	Rifabutin in RPMI + 10% FCS	Rifampicin in CA-MHB
HUMC1	0.002	32
HUMC1 ΔfhuE	2	32
UNT091-1	0.002	2
UNT091-1 ΔfhuE	0.5	4

Extended Data Fig 6. MIC of rifabutin and rifampicin on the *fhuE* deleted mutants and their parental strains.

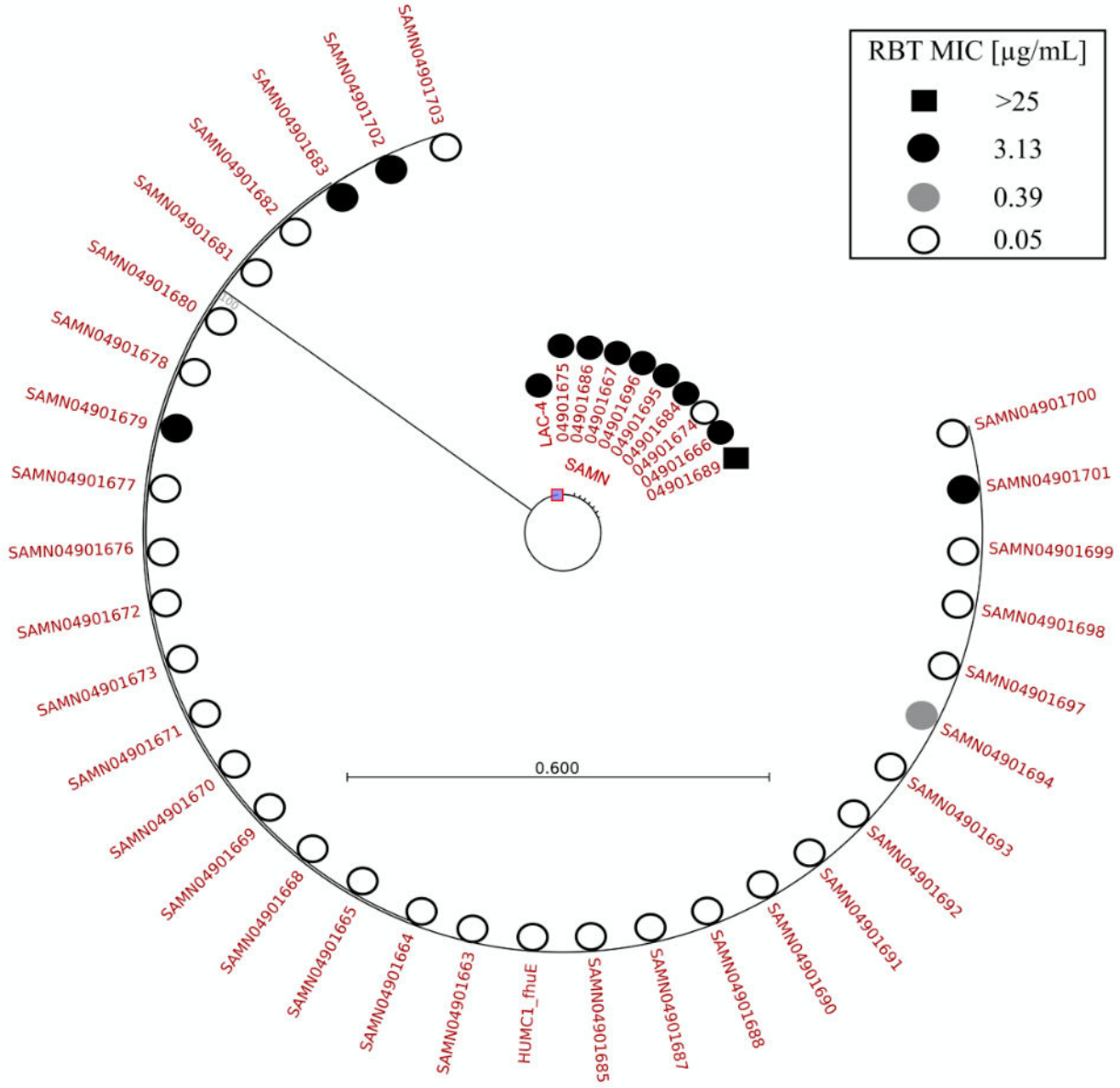

Extended Data Fig. 7. Clustering of fhuE by amino acid sequence.

MICs were done for 43 *A. baumannii* clinical isolates to determine if the isolates were hypersensitive to RBT in RPMI medium. 28 of the 33 isolates in the outer rings exhibit the hypersensitive phenotype (open circles) in RPMI (RBT MIC = 0.05 µg/mL). 9 of 10 isolates in the inner ring are not hypersensitive (filled-in shapes). Of the 41 carbapenem-resistant isolates tested, 26 of those are hypersensitive to RBT.

Strain	Plasmid	Rifabutin MIC (μg/mL)	
		MHII no IPTG	MHII 1 mM IPTG
A. baumannii ATCC 17978	no plasmid	4	4
	empty plasmid	1	2
	FhuE expressing plasmid	0.016	0.002

Extended Data Fig 8. MIC of rifabutin on the plasmid mediated *fhuE* expressing ATCC-17978 strains.

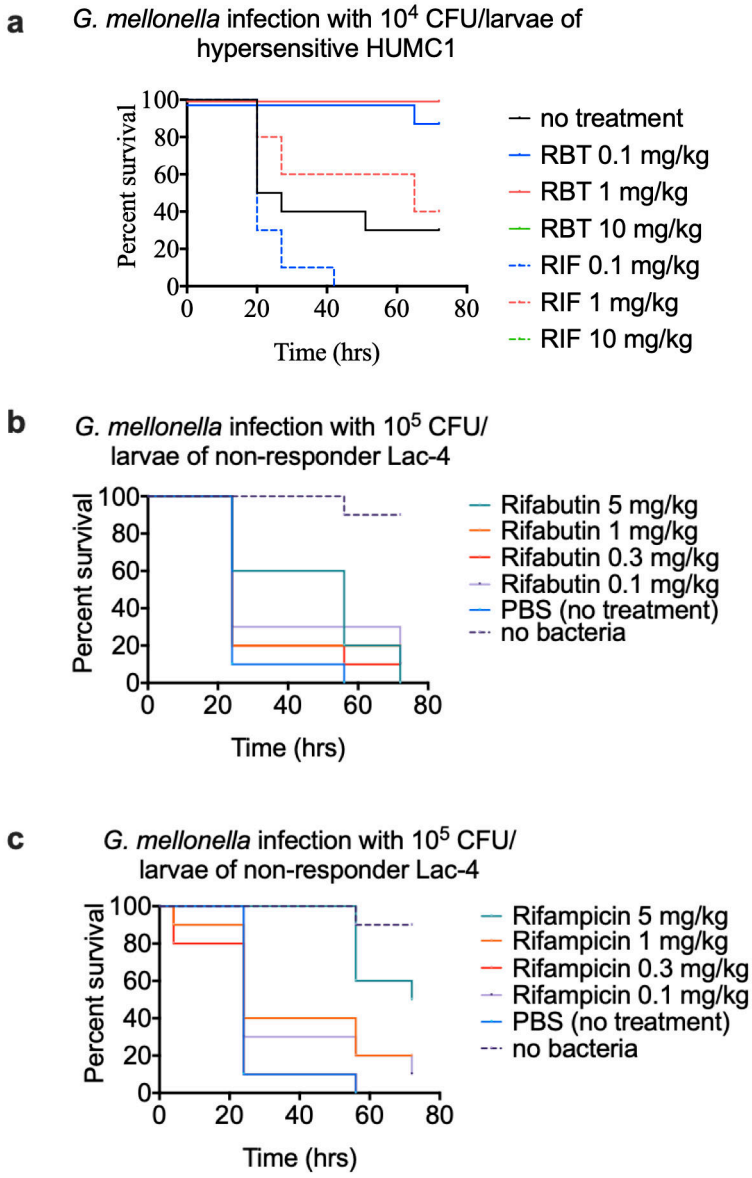

Extended Data Fig. 9. RPMI MIC predicts in vivo response to treatment.

Galleria mellonella larvae (10 per group) were infected with *A. baumannii.* **A)** Larvae were infected with strain HUMC1 at 1.6 x 10^4 cfu/larvae and treated with rifabutin (plain lines) or rifampicin (dashed lines) at 0.1 mg/kg (blue lines), 1 mg/kg (red lines) and 10 mg/kg (green lines) and survival was measured over 72 hours. **B)** *G. mellonella* larvae were infected with *A. baumannii* LAC-4 and treated with RBT or **C)** RIF. Consistent with the RPMI MIC data, there was no difference in outcomes based on treatment.

Strain	Drug	FICI	Result
HUMC1	rifabutin	0.46	synergy
	rifampin	0.58	no interaction
HUMC1 Δ*fhuE* mutant	rifabutin	0.46	synergy
	rifampin	0.46	synergy
LAC-4	rifabutin	0.46	synergy

Extended Data Fig 10- Drug -drug interaction between rifabutin or rifampin and colistin in MHII The drug-drug interaction were evaluated by calculating the fractional inhibitory concentration index (FICI).

FICI=FIC_A+ FIC_B=(C_A/MIC_A)+(C_B/MIC_B), in which C_A and C_B are drug concentration of drug A and drugB in combination and MIC_A and MIC_B are the MIC of drug A and drug B alone. Synergy was defined as FICI≤0.5, no interaction was defined as FICI >0.5–4.0 and antagonism was defined as FICI >4.0.

Supplementary Material

Refer to Web version on PubMed Central for supplementary material.

Acknowledgments:

We would like to thank Calibr's HTS and Compound Management teams for assisting with the ReFRAME screen. We would also like to thank Bill Weiss at UNT for supporting the neutropenic lung infection model.

Funding: This work was supported by National Institute of Allergy and Infectious Diseases (NIAID) (R01AI139052 to BL, RS, and BS; R01AI130060, R01AI117211 to BS); the Federal Drug Administration (FDA) (BAA Contract HHSF223201710199C to BL and BS); and Calibr at Scripps Research was supported by Bill & Melinda Gates Foundation (OPP1107194).

References

1. European Committee for Antimicrobial Susceptibility Testing (EUCAST) of the European Society of Clinical Microbiology and Infectious Diseases (ESCMID). Determination of minimum inhibitory concentrations (MICs) of antibacterial agents by broth dilution Clin Microbiol Infect. Blackwell Science Ltd; 2003 8 1;9(8):ix–xv.
2. Matuschek E, Brown DFJ, Kahlmeter G. Development of the EUCAST disk diffusion antimicrobial susceptibility testing method and its implementation in routine microbiology laboratories. Clin Microbiol Infect. 2014 4;20(4):O255–66. PMID: 24131428 [PubMed: 24131428]

3. Brown D, Canton R, Dubreuil L, Gatermann S, Giske C, MacGowan A, Martinez-Martinez L, Mouton J, Skov R, Steinbakk M, Walton C, Heuer O, Struelens MJ, Diaz Hogberg L, Kahlmeter G. Widespread implementation of EUCAST breakpoints for antibacterial susceptibility testing in Europe. Euro Surveill [Internet]. 2015 1 15;20(2). Available from: https://www.ncbi.nlm.nih.gov/pubmed/25613780 PMID: 25613780
4. Hombach M, Courvalin P, Böttger EC. Validation of antibiotic susceptibility testing guidelines in a routine clinical microbiology laboratory exemplifies general key challenges in setting clinical breakpoints. Antimicrob Agents Chemother. 2014 7;58(7):3921–3926. PMCID: PMC4068562 [PubMed: 24777093]
5. CLSI. Methods for Dilution Antimicrobial Susceptibility Tests for Bacteria That Grow Aerobically; Approved Standard—Ninth Edition. CLSI document M07-A9. Clinical and Laboratory Standards Institute;
6. Global priority list of antibiotic-resistant bacteria to guide research, discovery, and development of new antibiotics [Internet]. The World Health Organization; 2017 2 Available from: http://www.who.int/medicines/publications/WHO-PPL-Short_Summary_25Feb-ET_NM_WHO.pdf?ua=1
7. Fahnoe KC, Flanagan ME, Gibson G, Shanmugasundaram V, Che Y, Tomaras AP. Non-traditional antibacterial screening approaches for the identification of novel inhibitors of the glyoxylate shunt in gram-negative pathogens. PLoS One. 2012 12 11;7(12):e51732. PMCID: PMC3519852 [PubMed: 23240059]
8. Shlaes DM, Sahm D, Opiela C, Spellberg B. The FDA reboot of antibiotic development. Antimicrob Agents Chemother. 2013 10;57(10):4605–4607. PMCID: PMC3811409 [PubMed: 23896479]
9. Schäberle TF, Hack IM. Overcoming the current deadlock in antibiotic research. Trends Microbiol. 2014 4;22(4):165–167. PMID: 24698433 [PubMed: 24698433]
10. Centers for Disease Control (CDC). Antibiotic Resistance Threats in the United States, 2013. US Department of Health and Human Services, Centers for Disease Control and Prevention [Internet] 2013 4 23; Available from: http://www.cdc.gov/drugresistance/threat-report-2013/
11. Butler MS, Blaskovich MA, Cooper MA. Antibiotics in the clinical pipeline at the end of 2015. J Antibiot . 2017 1;70(1):3–24. PMID: 27353164 [PubMed: 27353164]
12. Tacconelli E, Carrara E, Savoldi A, Harbarth S, Mendelson M, Monnet DL, Pulcini C, Kahlmeter G, Kluytmans J, Carmeli Y, Ouellette M, Outterson K, Patel J, Cavaleri M, Cox EM, Houchens CR, Grayson ML, Hansen P, Singh N, Theuretzbacher U, Magrini N, WHO Pathogens Priority List Working Group. Discovery, research, and development of new antibiotics: the WHO priority list of antibiotic-resistant bacteria and tuberculosis Lancet Infect Dis. Elsevier; 2018 3;18(3):318–327. PMID: 29276051 [PubMed: 29276051]
13. Spellberg B, Guidos R, Gilbert D, Bradley J, Boucher HW, Scheld WM, Bartlett JG, Edwards J Jr, Infectious Diseases Society of America. The epidemic of antibiotic-resistant infections: a call to action for the medical community from the Infectious Diseases Society of America. Clin Infect Dis. 2008 1 15;46(2):155–164. PMID: 18171244 [PubMed: 18171244]
14. Janes J, Young ME, Chen E, Rogers NH, Burgstaller-Muehlbacher S, Hughes LD, Love MS, Hull MV, Kuhen KL, Woods AK, Joseph SB, Petrassi HM, McNamara CW, Tremblay MS, Su AI, Schultz PG, Chatterjee AK. The ReFRAME library as a comprehensive drug repurposing library and its application to the treatment of cryptosporidiosis. Proc Natl Acad Sci U S A. 2018 10 16;115(42):10750–10755. PMCID: PMC6196526 [PubMed: 30282735]
15. Nielsen TB, Pantapalangkoor P, Luna BM, Bruhn KW, Yan J, Dekitani K, Hsieh S, Yeshoua B, Pascual B, Vinogradov E, Hujer KM, Domitrovic TN, Bonomo RA, Russo TA, Lesczcyniecka M, Schneider T, Spellberg B. Monoclonal Antibody Protects Against Acinetobacter baumannii Infection by Enhancing Bacterial Clearance and Evading Sepsis. J Infect Dis. 2017 8 15;216(4):489–501. PMID: 28931235 [PubMed: 28931235]
16. Nielsen TB, Bruhn KW, Pantapalangkoor P, Junus JL, Spellberg B. Cryopreservation of virulent Acinetobacter baumannii to reduce variability of in vivo studies. BMC Microbiol. 2015 11 2;15:252. PMCID: PMC4630970 [PubMed: 26526621]
17. Bruhn KW, Pantapalangkoor P, Nielsen T, Tan B, Junus J, Hujer KM, Wright MS, Bonomo RA, Adams MD, Chen W, Spellberg B. Host fate is rapidly determined by innate effector-microbial interactions during Acinetobacter baumannii bacteremia. J Infect Dis. 2015 4 15;211(8):1296–1305. PMCID: PMC4447835 [PubMed: 25378635]

18. Luo G, Lin L, Ibrahim AS, Baquir B, Pantapalangkoor P, Bonomo RA, Doi Y, Adams MD, Russo TA, Spellberg B. Active and passive immunization protects against lethal, extreme drug resistant-Acinetobacter baumannii infection. PLoS One. 2012 1 10;7(1):e29446. PMCID: PMC3254619 [PubMed: 22253723]
19. Lin L, Tan B, Pantapalangkoor P, Ho T, Baquir B, Tomaras A, Montgomery JI, Reilly U, Barbacci EG, Hujer K, Bonomo RA, Fernandez L, Hancock REW, Adams MD, French SW, Buslon VS, Spellberg B. Inhibition of LpxC protects mice from resistant Acinetobacter baumannii by modulating inflammation and enhancing phagocytosis. MBio. 2012 10 2;3(5):e00312–12. PMCID: PMC3518917
20. Jacobs AC, Sayood K, Olmsted SB, Blanchard CE, Hinrichs S, Russell D, Dunman PM. Characterization of the Acinetobacter baumannii growth phase-dependent and serum responsive transcriptomes. FEMS Immunol Med Microbiol. 2012 4;64(3):403–412. PMID: 22211672 [PubMed: 22211672]
21. Blanchard C, Barnett P, Perlmutter J, Dunman PM. Identification of Acinetobacter baumannii serum-associated antibiotic efflux pump inhibitors. Antimicrob Agents Chemother. 2014 11;58(11):6360–6370. PMCID: PMC4249429 [PubMed: 25114126]
22. Asensio C, Pérez-Díaz JC. A new family of low molecular weight antibiotics from enterobacteria. Biochem Biophys Res Commun. 1976 3 8;69(1):7–14. PMID: 4071 [PubMed: 4071]
23. Thulin E, Thulin M, Andersson DI. Reversion of High-level Mecillinam Resistance to Susceptibility in Escherichia coli During Growth in Urine. EBioMedicine. 2017 9;23:111–118. PMCID: PMC5605379 [PubMed: 28855073]
24. Parquet MDC, Savage KA, Allan DS, Davidson RJ, Holbein BE. Novel Iron-Chelator DIBI Inhibits Staphylococcus aureus Growth, Suppresses Experimental MRSA Infection in Mice and Enhances the Activities of Diverse Antibiotics in vitro. Front Microbiol. 2018 8 14;9:1811. PMCID: PMC6103240 [PubMed: 30154764]
25. Parquet MDC, Savage KA, Allan DS, Ang MTC, Chen W, Logan SM, Holbein BE. Antibiotic-Resistant Acinetobacter baumannii Is Susceptible to the Novel Iron-Sequestering Anti-infective DIBI In Vitro and in Experimental Pneumonia in Mice. Antimicrob Agents Chemother [Internet]. 2019 9;63(9). Available from: 10.1128/AAC.00855-19 PMID: 31209004
26. Gallagher LA, Ramage E, Weiss EJ, Radey M, Hayden HS, Held KG, Huse HK, Zurawski DV, Brittnacher MJ, Manoil C. Resources for Genetic and Genomic Analysis of Emerging Pathogen Acinetobacter baumannii. J Bacteriol. 2015 6 15;197(12):2027–2035. PMCID: PMC4438207 [PubMed: 25845845]
27. Funahashi T, Tanabe T, Mihara K, Miyamoto K, Tsujibo H, Yamamoto S. Identification and characterization of an outer membrane receptor gene in Acinetobacter baumannii required for utilization of desferricoprogen, rhodotorulic acid, and desferrioxamine B as xenosiderophores. Biol Pharm Bull. 2012;35(5):753–760. PMID: 22687412 [PubMed: 22687412]
28. Durante-Mangoni E, Signoriello G, Andini R, Mattei A, De Cristoforo M, Murino P, Bassetti M, Malacarne P, Petrosillo N, Galdieri N, Mocavero P, Corcione A, Viscoli C, Zarrilli R, Gallo C, Utili R. Colistin and rifampicin compared with colistin alone for the treatment of serious infections due to extensively drug-resistant Acinetobacter baumannii: a multicenter, randomized clinical trial. Clin Infect Dis. 2013 8;57(3):349–358. PMID: 23616495 [PubMed: 23616495]
29. Payne DJ, Gwynn MN, Holmes DJ, Pompliano DL. Drugs for bad bugs: confronting the challenges of antibacterial discovery. Nat Rev Drug Discov. 2007 1;6(1):29–40. PMID: 17159923 [PubMed: 17159923]
30. El Zahed SS, Kumar G, Tong M, Brown ED. Nutrient Stress Small-Molecule Screening Platform for Escherichia coli. Methods Mol Biol. 2018;1787:1–18. PMID: 29736706 [PubMed: 29736706]
31. Zlitni S, Ferruccio LF, Brown ED. Metabolic suppression identifies new antibacterial inhibitors under nutrient limitation. Nat Chem Biol. 2013 12;9(12):796–804. PMCID: PMC3970981 [PubMed: 24121552]
32. Hermanson GT. Chapter 2 - Functional Targets for Bioconjugation Bioconjugate Techniques (Third edition). Boston: Academic Press; 2013 p. 127–228.
33. Eoh H, Rhee KY. Multifunctional essentiality of succinate metabolism in adaptation to hypoxia in Mycobacterium tuberculosis. Proc Natl Acad Sci U S A. 2013 4 16;110(16):6554–6559. PMCID: PMC3631649 [PubMed: 23576728]

34. Lee JJ, Lee S-K, Song N, Nathan TO, Swarts BM, Eum S-Y, Ehrt S, Cho S-N, Eoh H. Transient drug-tolerance and permanent drug-resistance rely on the trehalose-catalytic shift in Mycobacterium tuberculosis. Nat Commun. 2019 7 2;10(1):2928. PMCID: PMC6606615 [PubMed: 31266959]

35. Lee JJ, Lim J, Gao S, Lawson CP, Odell M, Raheem S, Woo J, Kang S-H, Kang S-S, Jeon B-Y, Eoh H. Glutamate mediated metabolic neutralization mitigates propionate toxicity in intracellular Mycobacterium tuberculosis. Sci Rep. 2018 5 31;8(1):8506. PMCID: PMC5981324 [PubMed: 29855554]

36. Trebosc V, Gartenmann S, Royet K, Manfredi P, Tötzl M, Schellhorn B, Pieren M, Tigges M, Lociuro S, Sennhenn PC, Gitzinger M, Bumann D, Kemmer C. A Novel Genome-Editing Platform for Drug-Resistant Acinetobacter baumannii Reveals an AdeR-Unrelated Tigecycline Resistance Mechanism. Antimicrob Agents Chemother. 2016 12;60(12):7263–7271. PMCID: PMC5119006 [PubMed: 27671072]

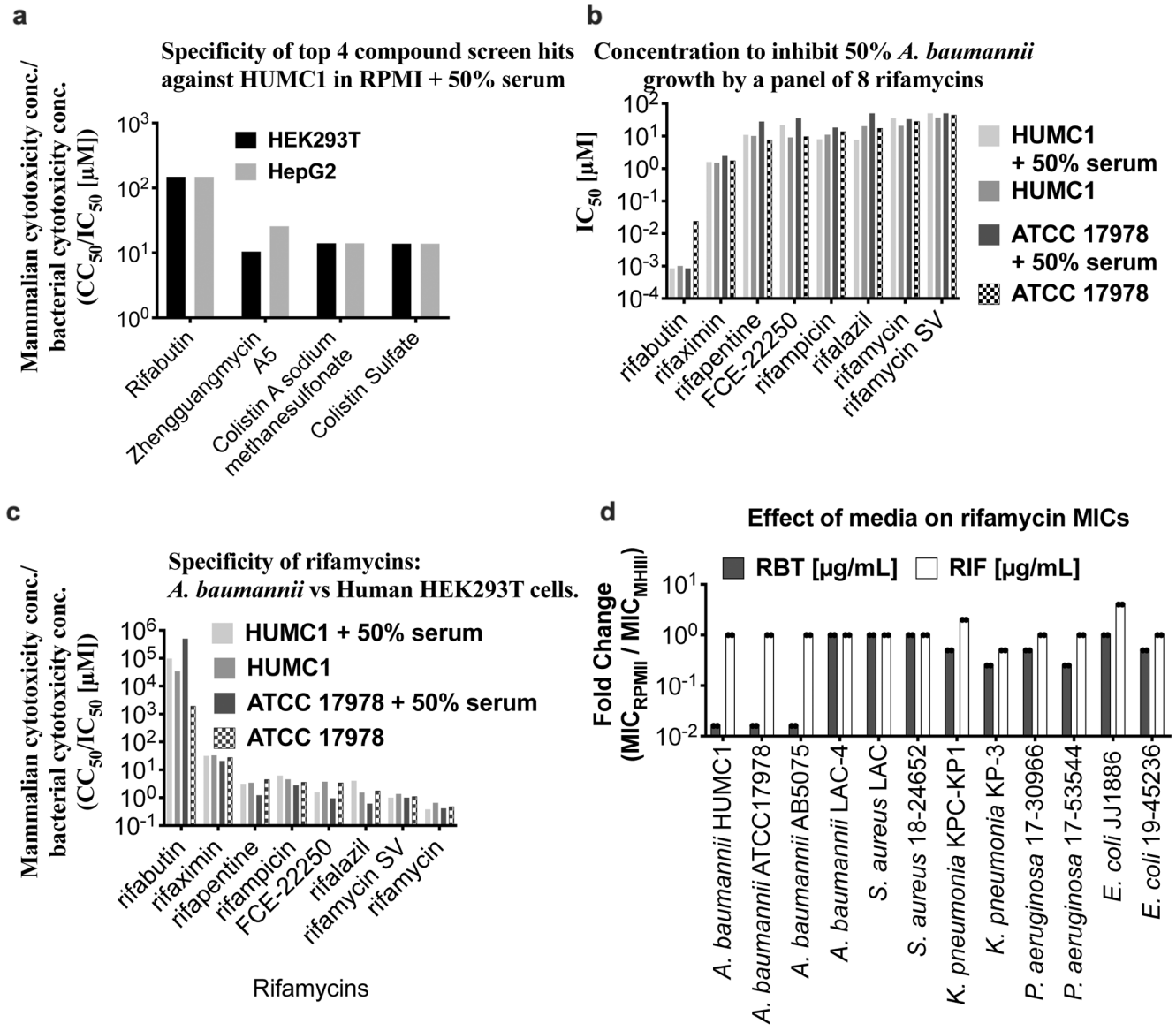

Figure 1- Summary of the ReFRAME library screen used for the identification of rifabutin.

11,862 small molecules were screened against *A. baumannii* ATCC 17978 (antibiotic-sensitive) and HUMC1 (extensively drug-resistant strains). **A)** Specificity (mammalian cell cytotoxicity / inhibition of bacteria growth; CC_{50} / IC_{50}) of the top 4 compound screen hits against *A. baumannii* HUMC1 and HEK293T and HepG2 mammalian cells. **B)** The IC_{50} was determined for 8 rifamycins. **C)** Specificity (mammalian cell cytotoxicity / inhibition of bacteria growth; CC_{50} / IC_{50}) of 8 rifamycins were tested against HEK293T mammalian cells and *A. baumannii* ATCC17978 andHUMC1 in RPMI with and without 50% serum. **D)** The fold change of MICs, when bacteria were cultured in RPMI or MHII, were determined for RBT and RIF against a panel of ESKAPE clinical isolates. One biological replicate of high throughput assays **(A-C)** were done in 3 technical replicates. MIC assays were repeated twice in duplicate.

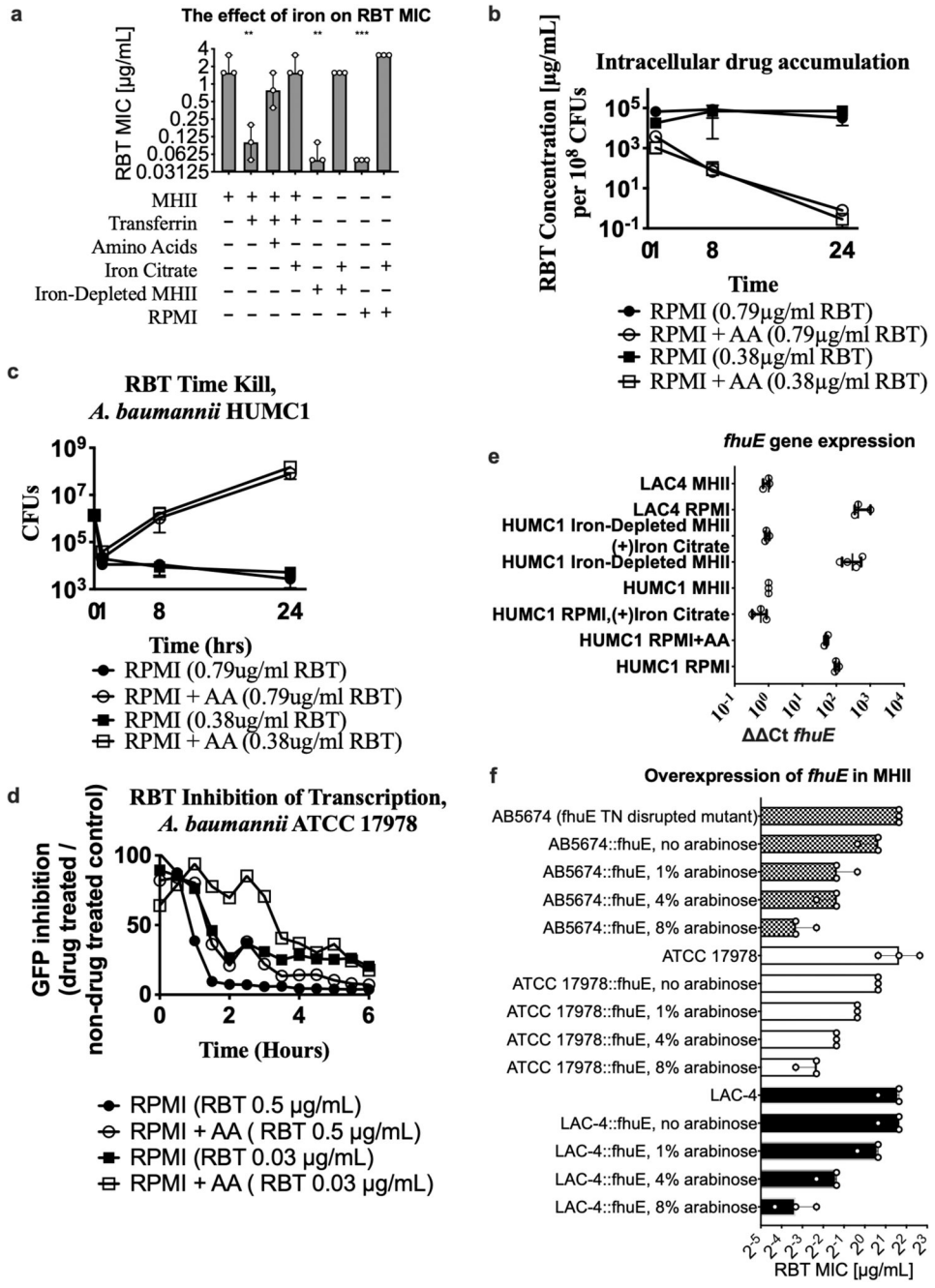

Fig. 2. The role of *fhuE* and sensitivity to RBT.

FhuE is predicted to be involved in iron transport. **A)** Iron was removed from MHII medium by the addition of transferrin or chelex to make the iron-depleted MHII formulation. The addition of 400 µM iron citrate to RPMI resulted in a greater MIC. All conditions (n=3 independent replicates) were tested against *A. baumannii* HUMC1. Statistical comparisons were determined by one-way ANOVA as compared to the MHII group. **B)** An overnight culture of *A. baumannii* HUMC1 was subcultured in fresh RPMI, with or without supplemented amino acids (AA). The intracellular concentration of RBT was measured by mass spectrometry and normalized to 1E8 CFUs (n=3 independent replicates); and **C)** The

number of viable cells was determined by plating serial dilutions on agar plates at 0, 1, 8, and 24 hours and enumerating CFUs (n=3 independent replicates). **D)** A GFP expressing reporter strain of *A. baumannii* ATCC17978 was cultured in RPMI, with or without supplemented amino acids, and challenged with RBT. The addition of amino acids (dashed lines) resulted in less inhibition of GFP fluorescence which is consistent with the higher MICs observed in these same conditions. The data is representative of 2 experiments. **E)** Expression of *fhuE* (n=3 independent replicates) was measured by qPCR (normalized to the housekeeping gene *rpo*D) in various culture conditions. **F)** $fhuE^{HUMC1}$ was cloned from *A. baumannii* HUMC1 (hypersensitive strain) in pVRL2Z under the control of an arabinose inducible promoter. MICs (n=3 independent replicates) were done with and without arabinose induction in MHII media. Median and interquartile ranges are plotted for panels **B, C, E, and F.**

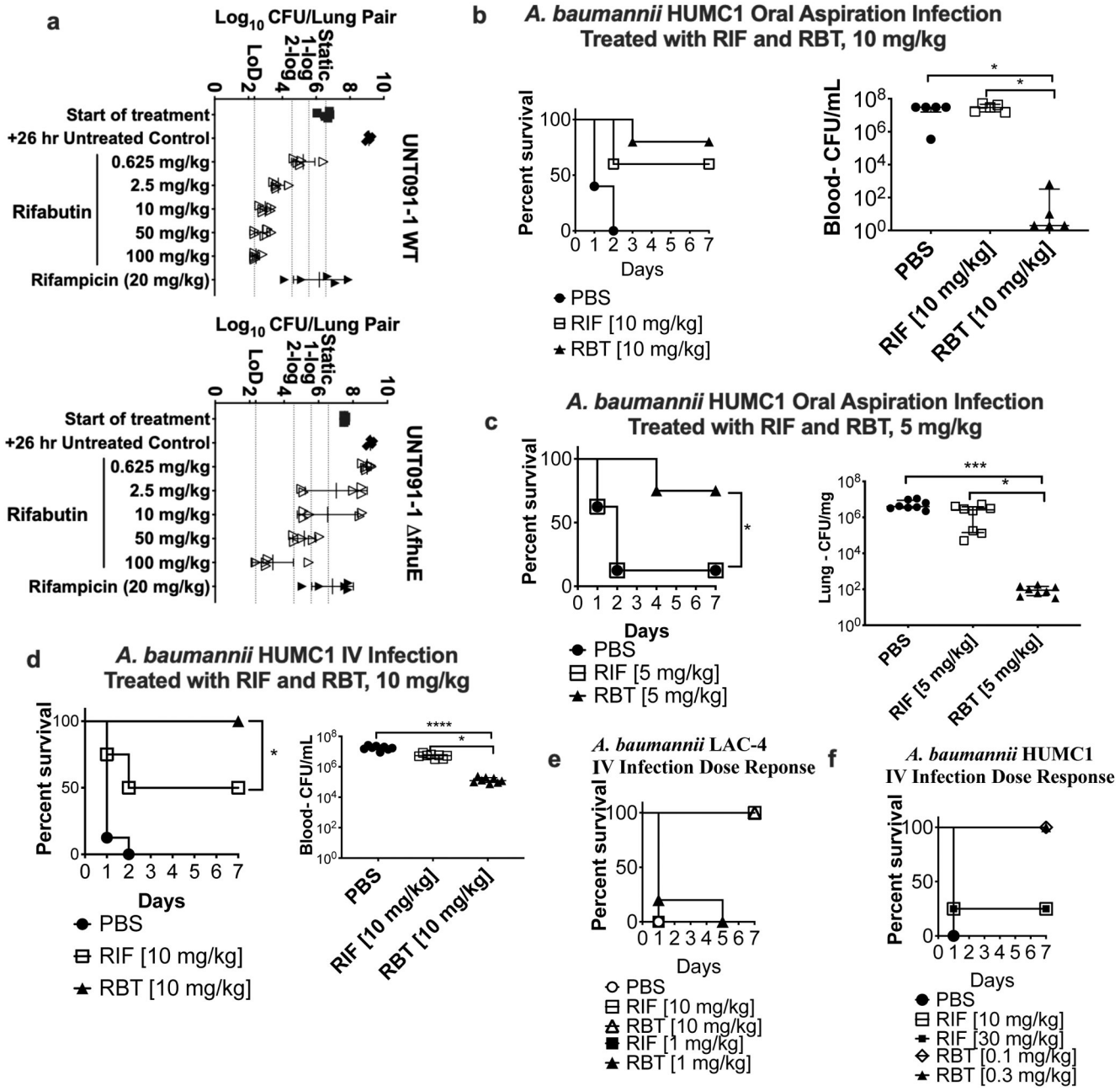

Fig 3. Efficacy of RBT *in vivo*.

Neutropenic, female CD-1 mice (n= 5) were inoculated intranasally (t = 0 hr) with equivalent titers (6.90 and 6.93 $\log_{10}$ CFU) of **A)** *A. baumannii* UNT091-1 wildtype and *A. baumannii* UNT091-1 Δ*fhuE* mutant. The treatment (single IV dose) was administered at 2-hour post-infection and bacterial burden was reported at 26 hours by determining CFU/lung. **B)** Immunocompetent C3H mice (n=5) were infected (oral aspiration pneumoniae model) with *A. baumannii* HUMC1 (carbapenem-resistant strain) and mice were treated with 10 mg/kg/daily for 3 days with RIF or RBT by oral gavage. Mice were monitored and euthanized when moribund (percent survival). At 24 hrs, blood was collected and there was

a significant reduction in CFUs and improved survival in the RBT treated group as compared to the PBS control group (Log-rank, p = 0.003; Kruskal-Wallis, p = 0.02). CFUs were significantly lower in RBT vs RIF treated groups (Kruskal-wallis, p=0.01). **C)** The experiment was repeated with a larger group of mice (n=8) and the dose was decreased to 5 mg/kg/daily for 3 days with RIF or RBT by oral gavage. Mice were monitored and euthanized when moribund (percent survival). Mice that received the RBT treatment had significantly lower CFUs compared to the PBS group (Kruskal-Wallis, p=0.0001) and the RIF treated group (Kruskal-Wallis, p=0.02) in the lung at 24 hrs post infection and survival was also significantly improved (Log-rank, p=0.005. **D)** C3H mice (n=8) were infected via tail vein injection with *A. baumannii* HUMC1. Mice were treated with 10 mg/kg/daily RIF or RBT for 3 days by oral gavage. RBT treatment improved survival (Log-rank, p<0.0001) and significantly reduced CFUs in the blood compared to PBS (Kruskal-Wallis, p<0.0001) and RIF groups (Kruskal-Wallis, p=0.047) at 1 hrs. The dotted grey lines signify a static, 1-log, or 2-log CFU reduction and the limit of detection (LOD). **E)** C3H mice (n=8) were infected with HUMC1 or **F)** LAC-4 IV and treated with RIF or RBT by oral gavage. Mice were monitored and euthanized when moribund (percent survival). Means and standard deviations are shown for panel **A.** Median and interquartile ranges are shown for panels **B-F.** P-values were determined using a Kruskal-Wallis and Dunn's multiple comparison test.

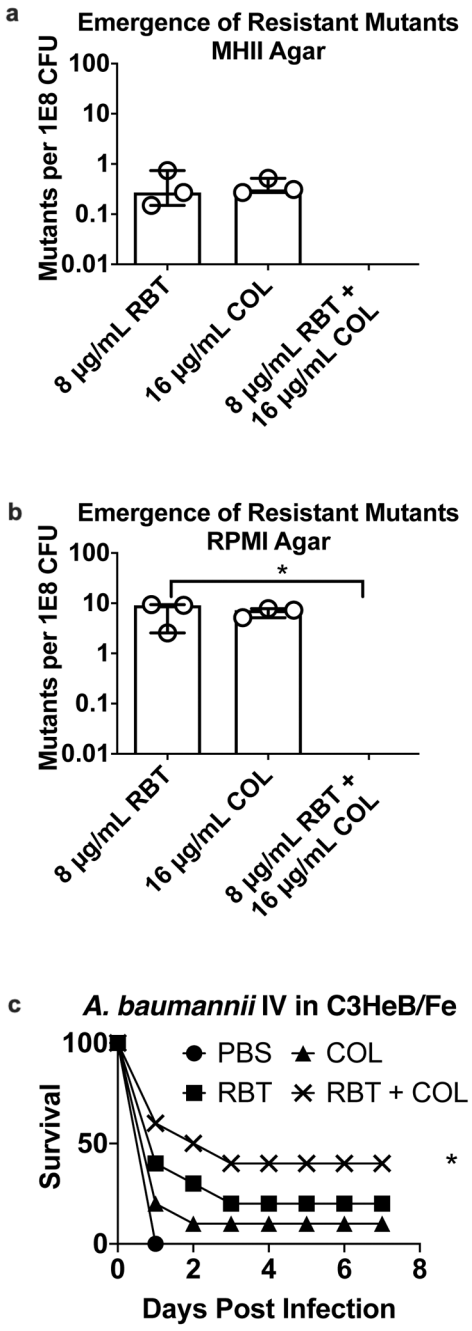

Fig. 4. RBT and COL combination therapy.

Selection of antibiotic resistant mutant by high inoculum plating. *A. baumannii* HUMC1 (n=3 independent replicates) was cultured in **A)** MHII or **B)** RPMI media overnight and mutants were selected by plating bacteria on drug plates containing 8 µg/mL of rifabutin, 16 µg/mL of colistin or the combination of both antibiotics. The addition of colistin is able to suppress the emergence of rifabutin resistance as compared to the PBS control group on RPMI agar (Kruskal-Wallis, p=0.046). Median and interquartile ranges are plotted. **C)** C3H mice (n=10 per group) were infected IV with *A. baumannii* HUMC1 IV and treated with subtheraptic doses of PBS, colistin (0.005 mg/kg) alone, rifabutin (0.05 mg/kg) alone, or the

combination of colistin + rifabutin. Mice were treated once daily for 3 days. Only the RBT + COL treatment group was significantly improved as compared to the PBS control group (Log-Rank, p=0.02).

Table 1:

MICs were performed against HUMC1 to determine which component of MHII inhibits the activity of RBT.

The MIC for CCCP and thioridazine alone are 8 and 64 μg/mL respectively.

	RBT MIC (μg/mL)	
	MHII	**RPMI**
Baseline	4.00	0.02
Temperature		
25 °C	4.00	0.05
Glucose Supplementation		
MHII + 200 mg/L glucose	2.00	-
MHII + 2,000 mg/L glucose	2.00	-
Modified RPMI		
5X RPMI	-	0.06
RPMI Supplemented with MHII	-	8.00
Efflux Pump Inhibitor		
CCCP (2 μg/mL)	1.56	-
thioridazine (8 μg/mL)	1.56	-
Verapamil (50 μg/mL)	1.56	-
Fractionated MHII Spiked Into RPMI		
10-30 kDa MHII Fraction	-	8.00
<10 kDa MHII Fraction	-	8.00
Acetonitrile Treated <10 kDa MHII Fraction		
Aqueous Layer	-	0.03
Organic Layer	-	4.00
Organic Layer, Proteinase K Digested	-	4.00
Organic layer, Sodium Periodate Treated	-	4.00
Amino Acid Supplementation RPMI		
Non-Essential Amino Acid Solution	-	0.78
Essential Amino Acid Solution	-	1.56
L-Arginine (0.5 mM)	-	0.05
Glutamic Acid (0.5 mM)	-	0.05
Glycine (0.5 mM)	-	0.05
Leucine (1 mM)	-	0.05
L-Histidine (0.5 mM)	-	1.56
L-Tryptophan (0.125 mM)	-	1.56
Iron Supplementation		
+ 400 μM iron citrate	3.13	3.13

Table 2-

Mutation Frequencies.

C3H mice were infected with 2.7 x 10^7 CFUs of *A. baumannii* HUMC1. Mice did not receive RIF or RBT treatments. Blood and kidneys were collected 16.5 hrs post infection and samples were plated on MHII or RPMI agar plates alone or supplemented with 8 μg/mL RIF or RBT.

RIF and RBT Mutation Frequency					
		BLOOD		**Kidney**	
Strain	**Media**	**RBT [8 μg/mL]**	**RIF [8 μg/mL]**	**RBT [8 μg/mL]**	**RIF [8 μg/mL]**
A. baumannii HUMC1	MHII	< 1.7E-9	8.4E-8	<3.7E-8	1.2E-7
A. baumannii HUMC1	RPMI	<8.3E-9	4.1E-7	3.7E-7	1.6E-6